1,3-Dipolar Cycloaddition of Nitrones to Free and Pt-Bound Nitriles. A Theoretical Study of the Activation Effect, Reactivity, and Mechanism

Maxim L. Kuznetsov,*,†,‡ Vadim Yu. Kukushkin,§ Andrei I. Dement'ev,‡ and Armando J. L. Pombeiro*,†

Centro de Química Estrutural, Complexo I, Instituto Superior Técnico, Av. Rovisco Pais, 1049-001 Lisbon, Portugal, Department of Chemistry, Moscow Pedagogical State University, 3, Nesvigskiy per., 119021 Moscow, Russian Federation, and Department of Chemistry, St. Petersburg State University, 198504 Stary Petergof, Russian Federation

Received: May 8, 2003; In Final Form: May 27, 2003

1,3-Dipolar cycloaddition of nitrones [H(R)C═N(CH_3)O] to nitriles— free and ligated to Pt^{II} and Pt^{IV} in the complexes *trans*-[$PtCl_2(NCCH_3)_2$] (**1**) and *trans*-[$PtCl_4(NCCH_3)_2$] (**2**)—was investigated by theoretical methods at different levels of theory, and the substituent and solvent effects have been studied. The activation of the nitriles upon coordination and the enhancement of their reactivity from the Pt^{II} to the Pt^{IV} complexes are interpreted in terms of kinetic (dramatic decrease of the activation barrier) and thermodynamic (increase of the absolute values of the reaction energies) viewpoints as well as of orbital (lowering of the π^*(CN) MO energy) and charge (increase of the charge on the β-C atom of RCN) control. The cycloaddition of nitrones occurs via a concerted mechanism for both free and coordinated nitriles rather than a stepwise mechanism. However, although the interaction with the uncoordinated RCN is nearly synchronous, the reaction with the complexes **1** and **2** is not only asynchronous but may be considered as of an intermediate type between the "conventional" synchronous cycloaddition (established for the free nitriles) and the nucleophilic addition to the β-C atom. The C-substituted nitrones are significantly less reactive than the nonsubstituted $H_2C{=}N(CH_3)O$ one, and the activation barriers of the aryl-substituted nitrones are higher than those of the C-alkyl nitrones. Replacement of the methyl by the phenyl group in the nitrile molecule RCN leads to a further promotion of its reactivity. The activation parameters and reaction energies have been calculated at different basis sets and levels of theory, up to MP4(SDTQ), CCSD(T), and CBS-Q. The activation energies are weakly sensitive to a change of the correlated methods. The consideration of the solvent effects results in the increase of the activation barriers, but the general trend of the change of the activation parameters in solution from free CH_3CN to **1** and **2** remains the same as that for the gas phase.

1. Introduction

1,3-Dipolar cycloaddition reactions play a paramount role for the synthesis of a great variety of heterocycles[1] including such pharmacologically important ones as tetrazoles, oxadiazoles, or oxadiazolines which can be obtained by coupling of azides (RNN≡N), nitrile oxides (RC≡NO), or nitrones (C(RR′)═N(R″)O) with organonitriles (RC≡N).[2] However, while the interaction of dipoles with various types of alkenes and alkynes has been investigated extensively,[1,3] the cycloaddition to nitriles, as dipolarophiles, is relatively poorly explored. A main problem with the use of nitriles for the 1,3-dipolar cycloadditions is the low reactivity of noncoordinated RCN unless a strong electron acceptor R group is used. Hence, to proceed smoothly, these reactions have to be catalyzed or promoted by Lewis acids, for example, metal ions. The activation effect is usually reached by two ways, that is, interaction of the Lewis acid either with the dipolarophile or with the dipole species. Qualitative considerations in terms of the frontier molecular orbital (FMO) theory[4] allow the interpretation of such activation by lowering of the FMO energies of the dipolarophile, in the former case (normal electron-demand reactions), or of the dipole, in the latter case (inverse electron-demand reactions), upon their ligation to the Lewis acid. As a result, the HOMO−LUMO gap for the interacting orbitals of the reactants decreases favoring the cycloaddition.[3]

Thus, for both normal and inverse electron-demand reactions, the selective coordination of the Lewis acid *to one of the reagents* is important, since otherwise the concurrent (but not necessarily the same in absolute value) lowering of the FMO energies of *both reactants* should lead to a lower activation than in the selective complexation. The selectivity is often related to the hardness of the donor and acceptor centers. Usually, the cycloaddition reactions are catalyzed by hard or borderline acids, for example, Ti^{IV}, Mg^{II}, Ln^{III}, Al^{III}, Ni^{II}, and Cu^{II} [5] whereas, for the normal electron-demand cycloaddition to nitriles (the subject of our previous experimental studies[6−8]), the soft metal centers are expected to be effective. Currently, there are only several examples of cycloadditon reactions with RCN that have been promoted by soft metal ions, for example, Pt^{II}, Pd^{II}, Rh^{I}, Ir^{I}, or Au^{I} for the cycloaddition of azides to nitriles[2] and Pt^{II} or Pt^{IV} for the nitrone or nitrile oxide cycloadditon.[6−8]

In our previous works, the activation of nitriles by the soft Pt^{II} and Pt^{IV} centers in the complexes *trans*-[$PtCl_2(NCR)_2$] and

---

* To whom correspondence should be addressed. Fax: +351-21-846-4455; e-mail: pombeiro@ist.utl.pt.

† Instituto Superior Técnico.

‡ Moscow Pedagogical State University.

§ St. Petersburg State University.

10.1021/jp035261k CCC: $25.00

SCHEME 1: Cycloaddition of Nitrile Oxides and Nitrones to Pt-Bound Nitriles

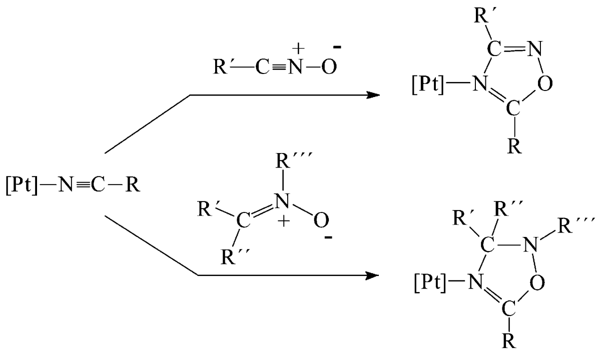

[Pt] = $PtCl_2(NCR)$, $PtCl_4(NCR)$

trans-$[PtCl_4(NCR)_2]$ toward the nitrile oxide[8] or nitrone[6,7] cycloaddition to give the 1,2,4-oxadiazole and Δ^4-1,2,4-oxadiazoline platinum complexes (Scheme 1) was examined experimentally. It was shown that while the 1,3-dipoles do not react with free RCN (R = alkyl), the ligation of nitriles to Pt^{IV} provides an easy and effective promotion of the reactions. An effect of the metal oxidation state was found, the nitriles at Pt^{IV} reacting much faster than when bound to Pt^{II}. In *trans*-$[PtCl_4(NCR)_2]$, the nature of the R group in RCN does not affect significantly the reaction whereas for *trans*-$[PtCl_2(NCR)_2]$ the increase of the electron acceptance of R (e.g., use of the phenyl group instead of an electron-donor alkyl one) facilitates the reaction noticeably, demonstrating the importance of the nature of R for the reactivity of RCN.

The present work, being a continuation of our previous experimental studies, is the first attempt of an extended theoretical investigation of the nitrone-to-nitriles cycloaddition and of the activation effect of the “nitrilophilic” electron-poor metal centers (Pt^{II} and Pt^{IV}) which activate only the nitrile without affecting the dipole. A main goal of this work is to provide *quantitative* estimates of the *qualitative* effects observed experimentally and to interpret the platinum activation effect on the ligated nitriles, the trends in their reactivity, and its dependence on both the metal oxidation state and the nature of the organic groups in the nitrile and nitrone molecules. To achieve this goal, a detailed search of the possible mechanisms of the reactions of nitrones (mainly the *N*-methyl nitrone, $H_2C{=}N(CH_3)O$, taken as the simplest model) with nitriles, free and bound to Pt^{II} (in *trans*-$[PtCl_2(NCCH_3)_2]$, **1**) or Pt^{IV} (in *trans*-$[PtCl_4(NCCH_3)_2]$, **2**), has been carried out. The driving forces of the activation of the nitriles in the complexes are discussed, and a comparative analysis of the energetic characteristics of the reactions (calculated at different levels of theory, including the estimate of the solvent and substituent effects) was performed.

This article has the following structure. First, we describe the energetic characteristics and the composition of the frontier MOs of the reactants as well as the calculated structural parameters of the final products and discuss the reactivity in terms of the qualitative FMO theory. Second, the concerted pathway of the reaction is examined in detail including (i) the comparative analysis of the mechanistic features and the nature of the transition states for the reaction of free acetonitrile and the platinum nitrile complexes at the B3LYP/6-31G* level; (ii) the discussion of the energetic parameters of the reaction calculated at different levels of theory, up to MP4(SDTQ), CCSD(T), and CBS-Q; and (iii) the analysis of the solvent and substitution effects on the energetic characteristics of the reactions. Third, the possibility of the stepwise mechanism is also considered.

2. Computational Details

The full geometry optimization of all structures and transition states has been carried out in Cartesian coordinates with help of the Gaussian-98[9] and GAMESS[10] program packages. The structures of acetonitrile, *N*-methyl nitrone, final products of their cycloaddition, corresponding transition states (TS), and orientation complexes (OC) have been optimized at the HF, DFT, and MP2[11] levels of theory using standard basis sets of Gauss functions 6-31G, 6-31G*, and 6-31+G**.[12] The DFT calculations have been performed using Becke’s three-parameter hybrid exchange functional[13] in combination with the gradient-corrected correlation functional of Lee et al.[14] (B3LYP). Single-point calculations of all these structures have been carried out at the HF, B3LYP, MP2, MP3, MP4(SDTQ), and CCSD(T) (coupled cluster with single and double excitations and a perturbative estimate of triple excitations[15]) levels using 6-311++G**,[16] 6-31+G**, or 6-31G* basis sets (see the section Results and Discussion and tables). Finally, these structures have been computed using the Complete Basis Set method of Petersson and co-workers[17] at the CBS-Q level.[17f]

The structures of the C-substituted nitrones, PhCN, platinum complexes, corresponding final products, TSs, and OCs have been optimized at the B3LYP level which was found as the most reasonable one for the investigation of the nitrone-to-nitrile cycloaddition taking into account the low computational cost of this method and the fact that the results obtained at B3LYP agree well with those calculated at the higher correlated methods (see Results and Discussion). A quasi-relativistic Stuttgart pseudopotential described 60 core electrons and the appropriate contracted basis set (8s7p6d)/[6s5p3d][18] for the platinum atom and the 6-31G* basis set for other atoms were used. Further, this level is denoted as B3LYP/6-31G* even for the Pt-complexes despite the usage of the other basis set on the Pt atom. Symmetry operations were not applied for all structures. For the stepwise mechanism, the calculations of the possible singlet dipolar, singlet, and triplet biradical intermediates and transition states of the Michael-type have been performed at the UB3LYP/6-31G* and GVB−PP(1)/6-31G* levels, the latter used for the location of possible singlet biradical structures. The stability of the Hartree−Fock and DFT solutions for the equilibrium geometries was tested using the keyword STABLE in Gaussian-98.

The Hessian matrix was calculated numerically (for HF) or analytically (for B3LYP) for all optimized structures to prove the location of correct minima (no imaginary frequencies) or saddle points (only one negative eigenvalue), and to estimate the zero-point energy correction and thermodynamic parameters, the latter were calculated at 25 °C. The intrinsic reaction coordinate (IRC) was also calculated at the HF/6-31G* level (for the reaction of $H_2C{=}N(CH_3)O$ with CH_3CN, **1** and **2**) and at the B3LYP/6-31G* level (for the reaction of $H_2C{=}N(CH_3)O$ with free CH_3CN) by the Gonzalez−Schlegel method.[19] The calculations were started from the saddle points found at the respective approach to the direction in which the largest magnitude component of the imaginary normal mode is positive and to the opposite direction. The structures of the orientation complexes found as a result of these calculations have been reoptimized at all above-mentioned levels.

The Wiberg bond indices[20] for the transition states have been computed by using the natural bond orbital (NBO) partitioning scheme.[21] The synchronicity of the reactions has been calculated using the formula reported previously.[22,23] The bonding nature in the TSs has been studied with the help of the AIM method of Bader.[24] For the calculations of the electron density distribution $\rho(\mathbf{r})$, the gradient vector field $\nabla\rho(\mathbf{r})$, and its associated Laplacian $\nabla^2\rho(\mathbf{r})$, the programs GRIDV, GRDVEC, CONTOR, and EXT94B were used.[25]

Because of the presence of the van der Waals orientation complexes which are formed at the initial steps of the reaction, counterpoise estimates of basis set superposition error (BSSE)[26] were made for the reaction of $H_2C{=}N(CH_3)O$ with CH_3CN, **1**, and **2** by performing calculations on the nitrone and acetonitrile or the complexes including basis functions from the other reactant, in the orientation complex geometries.

Solvent effects were taken into account for the estimate of the energetic characteristics of the *N*-methyl nitrone cycloaddition to CH_3CN, **1**, and **2** at the B3LYP/6-31G* level by using the polarizable continuum model[27] in the CPCM version[28] with CH_2Cl_2 as a solvent. For the reaction of free nitrile, the full geometry optimization at this level has been performed while, for the reaction of the complexes, the single-point CPCM calculations based on the gas-phase geometry have been carried out.

3. Results and Discussion

Owing to their high basic and applied significance, the cycloaddition reactions in general[29,30] and the 1,3-dipolar cycloadditions[29,31] in particular have been the object of extensive theoretical investigations which, in the latter case, include studies on cycloaddition of such dipoles as fulminic acid, nitrile oxides,[23,32] nitrones,[23,32k,33] nitronates,[34] azomethine ylides,[35] diazomethane,[32e] 1,3-heterocumulenes (these compounds can be also assigned as dipoles when the polar resonance structures are considered),[36] ozone,[37] or allyl anions[38] to alkenes and alkynes. However, to the best of our knowledge, the cycloaddition to nitriles was not theoretically studied at all despite the possibility to use these reactions for the synthesis of important heterocycles such as oxadiazolines and oxadiazoles.

For the 1,3-dipolar cycloaddition, two general plausible mechanisms are usually considered, that is, concerted[31a,39] and stepwise[40] ones. The former proceeds with formation of one transition state and may be synchronous or asynchronous depending on whether the two new contacts between the reacting molecules in the transition state have the same bond orders and extensions or not. The stepwise route starts with the one-end addition of a dipole to give a dipolar or diradical intermediate or transition state, whereupon the ring closure terminates the reaction. The concerted mechanism is supported in most of the publications[23,31a,32c,e,i,k,l,33a,c,e,f,34,35a,36] and there are only a few works[32j,33b,35b,38] which suggest that the stepwise mechanism is the more preferable one. Following the plan given in the Introduction, we first discuss the interaction of nitrones with nitriles in terms of the FMO theory.

Equilibrium Structures and MO Composition of the Reactants. As preliminary steps of the theoretical study, the equilibrium geometries of the reactants, that is, *N*-methyl nitrone ($H_2C{=}N(CH_3)$-O) and acetonitrile ($CH_3C{\equiv}N$), taken as the simplest models, have been calculated at different levels and basis sets (see Computational Details). The geometry optimization of the complexes *trans*-$[PtCl_2(NCCH_3)_2]$ **1** and *trans*-$[PtCl_4(NCCH_3)_2]$ **2** as well as the analysis of the composition of their FMOs at the HF, MP2, and B3LYP levels of theory have been performed previously,[41] and selected B3LYP bond lengths are included in Table 1 for comparison with those of the other systems of the current study. The main calculated bond lengths of nitrone and acetonitrile are available from the authors upon request.

TABLE 1: Selected Bond Lengths (Å) for the Starting Complexes 1 and 2, Products of the Nitrone Cycloaddition (3−5, 9−13), and the Transition States (TS1−TS8) Calculated at the B3LYP/6-31G* Level

	1	**2**	**3**	**4**
Pt−Cl	2.369	2.394		2.368−2.374
Pt−N(1)	1.963	1.975		2.023
N(1)−C(2)	1.152	1.148	1.273	1.288
C(2)−C(3)	1.455	1.454	1.493	1.488
C(2)−O(5)			1.370	1.344
N(4)−O(5)			1.472	1.482
N(1)−C(6)			1.461	1.474
N(4)−C(7)			1.465	1.469
N(4)−C(6)			1.490	1.473

	5	**9**	**10**	**11**
Pt−Cl	2.391−2.397			
Pt−N(1)	2.036			
N(1)−C(2)	1.296	1.273	1.272	1.273
C(2)−C(3)	1.486	1.493	1.493	1.493
C(2)−O(5)	1.341	1.369	1.369	1.369
N(4)−O(5)	1.482	1.470	1.467	1.467
N(1)−C(6)	1.487	1.465	1.469	1.469
N(4)−C(7)	1.469	1.464	1.464	1.464
N(4)−C(6)	1.463	1.501	1.494	1.495
C(6)−C(8)		1.527	1.525	1.525

	12	**13**	**TS1**	**TS2**
Pt−Cl				2.369−2.382
Pt−N(1)				1.996
N(1)−C(2)	1.277	1.278	1.197	1.205
C(2)−C(3)	1.470	1.470	1.476	1.484
C(2)−O(5)	1.374	1.372	1.935	1.700
N(4)−O(5)	1.469	1.464	1.326	1.336
N(1)−C(6)	1.459	1.466	2.066	2.388
N(4)−C(7)	1.466	1.465	1.465	1.464
N(4)−C(6)	1.488	1.494	1.328	1.305
C(6)−C(8)		1.526		

	TS3	**TS4**	**TS5**	**TS6**
Pt−Cl	2.387−2.405			
Pt−N(1)	1.980			
N(1)−C(2)	1.193	1.198	1.201	1.201
C(2)−C(3)	1.478	1.477	1.479	1.480
C(2)−O(5)	1.770	1.919	1.869	1.863
N(4)−O(5)	1.327	1.330	1.337	1.339
N(1)−C(6)	2.533	2.081	2.092	2.097
N(4)−C(7)	1.468	1.464	1.464	1.464
N(4)−C(6)	1.294	1.337	1.345	1.346
C(6)−C(8)		1.499	1.472	1.469

	TS7	**TS8**
N(1)−C(2)	1.200	1.205
C(2)−C(3)	1.453	1.457
C(2)−O(5)	1.976	1.885
N(4)−O(5)	1.322	1.336
N(1)−C(6)	2.057	2.088
N(4)−C(7)	1.464	1.464
N(4)−C(6)	1.327	1.346
C(6)−C(8)		1.468

Following the classification of Sustmann,[42] the cycloaddition reactions can be classified in any of the following three groups according to the type of the HOMO−LUMO interaction of the dipole and the dipolarophile molecules. Group I includes the reactions that are controlled by the $\text{HOMO}_{\text{dipole}}$−$\text{LUMO}_{\text{dipolarophile}}$ interaction, whereas the reactions of group III are determined by the mixing of the $\text{HOMO}_{\text{dipolarophile}}$ and the $\text{LUMO}_{\text{dipole}}$. For the reactions of group II, both types of the HOMO−LUMO interactions take place. The 1,3-dipolar cycloaddition of nitrones is usually considered as a reaction of the type II.[3] Indeed, our calculations of $H_2C{=}N(CH_3)O$ and noncoordinated CH_3CN

SCHEME 2: Interaction of the π(CN) or $\pi^*_{d-\pi(L)}$ and π^*(CN) Orbitals of RCN, 1, and 2 with the Corresponding LUMO and HOMO of Nitrones (H(R′)C=N(CH$_3$)O) for B3LYP/6-31G* Level

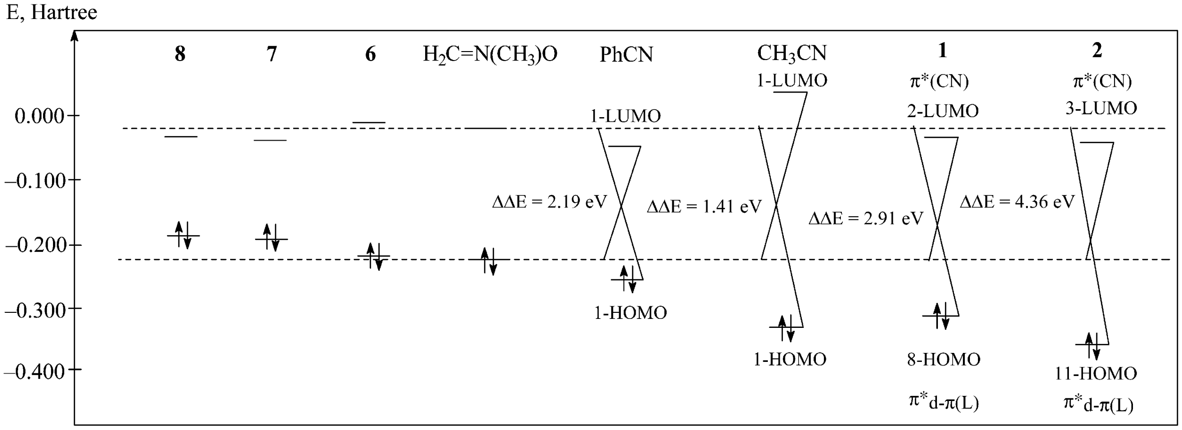

suggest that the difference of the two HOMO−LUMO energetic gaps ($\Delta\Delta E$, Scheme 2) is in the range of 0.9−3.3 eV indicating that both HOMO$_{\text{nitrile}}$–LUMO$_{\text{nitrone}}$ and HOMO$_{\text{nitrone}}$–LUMO$_{\text{nitrile}}$ types of interactions occur for the reaction of the free nitrile, although the latter prevails over the former one.

As it was shown,[41c] the coordination of the nitriles to Pt$^{\text{II}}$ and Pt$^{\text{IV}}$, in complexes **1** and **2**, leads to the energetic lowering of the LUMOs which contain the π^*(CN) orbitals (Scheme 2, Figure 1). The energies of the HOMOs bearing the π(CN) MOs also decrease for **2** in comparison with free CH$_3$CN. As a result, the HOMO$_{\text{nitrone}}$–LUMO$_{\text{nitrile}}$ gap is reduced from CH$_3$CN to **1** and further to **2** but the HOMO$_{\text{nitrile}}$–LUMO$_{\text{nitrone}}$ difference for **2** is even higher than for free CH$_3$CN. Thus, the qualitative consideration of the FMO composition suggests that the 1,3-cycloaddition of nitrones to the bound nitriles are determined mostly by the HOMO$_{\text{nitrone}}$–LUMO$_{\text{nitrile}}$ interaction, being a normal electon-demand reaction, and the activation of the ligands can be interpreted in terms of frontier MO arguments as the result of the lowering of the π^*(CN) MO energy upon coordination.

Equilibrium Structures of the Cycloaddition Products. The equilibrium structures of the products of the cycloaddition of *N*-methyl nitrone to free acetonitrile and to the complexes **1** and **2**, that is, $\overline{N{=}C(CH_3)ON(CH_3)CH_2}$ (**3**) and *trans*-[PtCl$_n$(MeCN){$\overline{N{=}C(CH_3)ON(CH_3)CH_2}$}] ($n$ = 2, **4**; n = 4, **5**) (Figure 2 and Table 1), have been calculated at the B3LYP/6-31G* level. The $\overline{N{=}C(C)ONC}$ fragments are not completely planar, the displacement of the N(4) atom from the N(1)C(2)O(5)C(6) plane is ca. 0.2−0.4 Å, and this atom has pyramidal surroundings because of the presence of the lone electron pair. For complex **4**, the N(1)C(2)O(5)C(6) plane forms an angle of ca. 65° with that defined by the Pt, Cl, and N(1) atoms, which agrees with the X-ray data for *trans*-[PtCl$_2${$\overline{N{=}C(CH_3)ON(CH_3)C}$(Ph)H}$_2$][7] (the X-ray dihedral angles are 68.2° and 57.9°). The plane of the organic cycle in **5** is situated between the Cl atoms, also being consistent with the experimental data for *trans*-[PtCl$_4${$\overline{N{=}C(CH_3)ON(CH_3)C}$-($p$-C$_6H_4OCH_3$)H}$_2$].[6]

Only three experimental X-ray structures of noncoordinated Δ^4-1,2,4-oxadiazolines are known,[43] and the bond lengths calculated for **3** are in perfect agreement with the experimental parameters for 2-(7-cyanonorcaran-7-yl)-5-(ethoxycarbonyl)-4,5,6,11b-tetrahydro-(Δ^4-1,2,4-oxadiazolino)(2,3-a)-β-carboline[43a] with the maximum deviation of 0.016 Å for the N(1)C(6) bond. The maximum difference between the main calculated bond lengths for **4** and **5** and the respective X-ray experimental

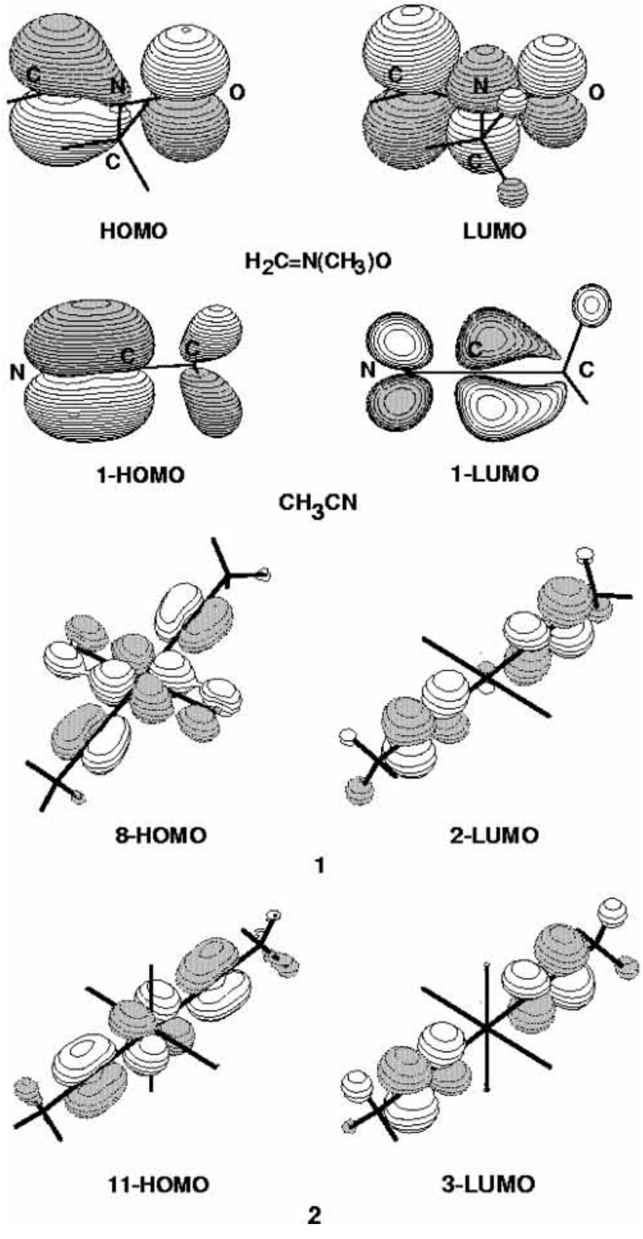

Figure 1. Plots of selected HOMOs and LUMOs determining the nitrone-to-nitrile cycloaddition.

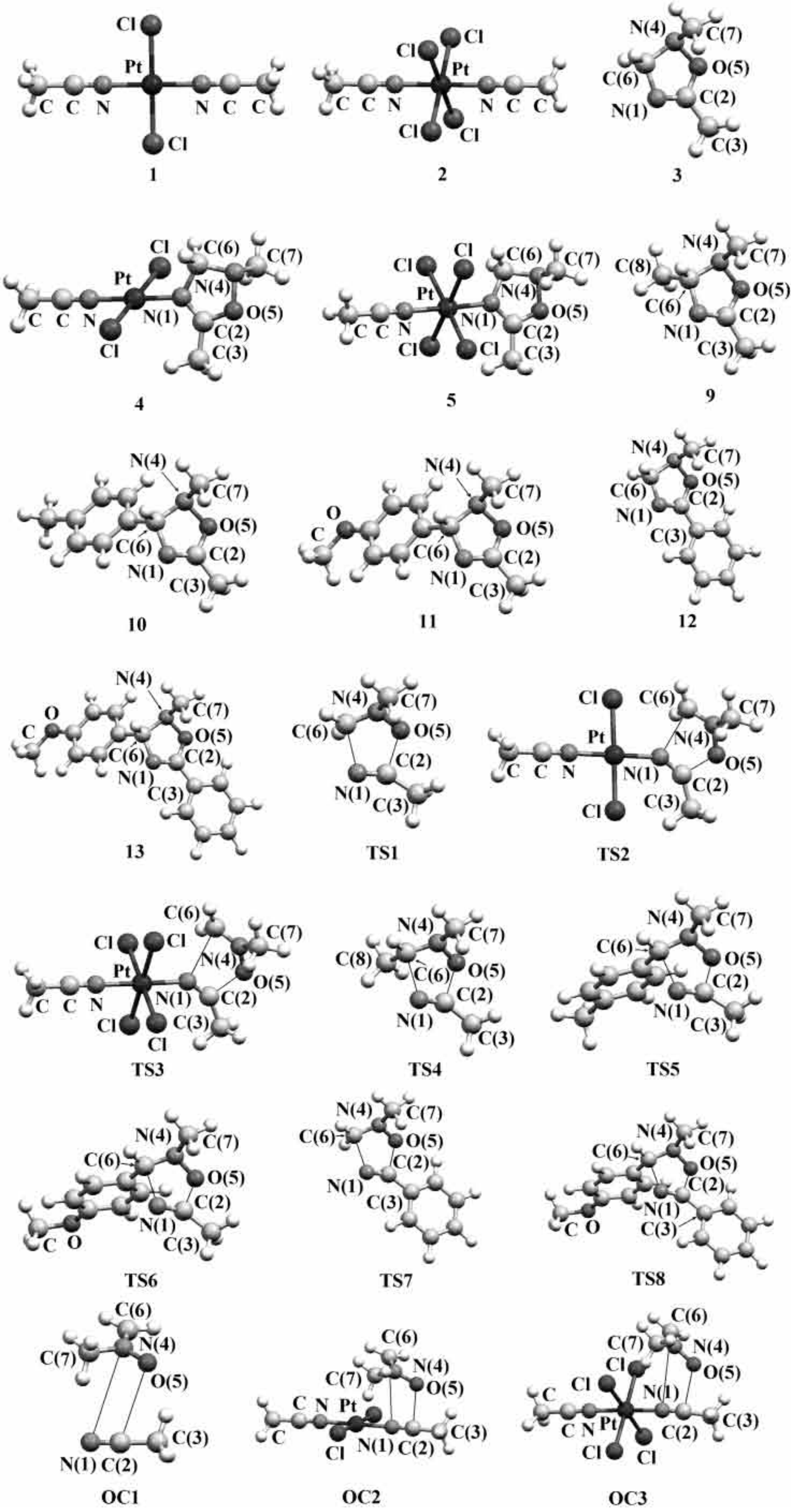

Figure 2. Equilibrium geometries of starting nitrile complexes (**1**, **2**), products of cycloaddition (**3**−**12**), transition states (**TS1**−**TS8**), and orientation complexes (**OC1**−**OC3**).

parameters for *trans*-[$\mathrm{PtCl_2\{\overline{N{=}C(CH_3)ON(CH_3)C}(Ph)H\}_2}$] and *trans*-[$\mathrm{PtCl_4\{\overline{N{=}C(CH_3)ON(CH_3)C}(\mathit{p}\text{-}C_6H_4OCH_3)H\}_2}$]^{6,7} was detected for the Pt−Cl bonds (0.066−0.077 Å) and the N(1)C(2) bond for **5** (0.032 Å) and is not higher than 0.019 Å for the other bonds, often appearing within the 3σ interval of the experimental data.

Concerted Mechanism. (i) Gas-Phase Transition States. For the *concerted* nitrone-to-nitrile cycloaddition, one TS was located for each process at the B3LYP/6-31G* level (**TS1**, **TS2,** and **TS3**, Figure 2). The N(1)−C(2) distance and the corresponding bond order have intermediate values in TSs in comparison with those for the reagents and the products whereas the N(4)−C(6) distance in **TS2** and **TS3** is even shorter than that in the initial nitrone. The N(4)−O(5) and Pt−N(1) bonds are generally elongated from the reactants to the TSs and then to the final species. The NPA charge transfer from the nitrone to nitrile molecules upon formation of **TS1** is small (0.06 e) but increases noticeably for **TS2** (0.28 e) and **TS3** (0.33 e) reflecting the increased electron deficiency of the nitrile molecule from CH_3CN to **1** and **2** and correlating with the enhancement of the reactivity along this sequence.

The "imaginary frequencies" of the TSs have small values and they decrease from **TS1** to **TS3** (450i, 268i, and 143i for **TS1**, **TS2**, and **TS3**, respectively), which correlates with the growth of the asynchronicity along this sequence (see below). Vectors associated with these imaginary frequencies correspond to the approach of the $H_2CN(CH_3)O$ and CH_3CN fragments to form two new C(2)O(5) and N(1)C(6) bonds and to further bending of the acetonitrile ligand that results in the final formation of the cycloaddition products **3**−**5** if the movement to the product's basin occurs.

The **TS1** corresponds to the concerted almost *synchronous* pathway despite that the N(1)···C(6) internuclear distance is 0.131 Å longer than the C(2)···O(5) one. Indeed, the calculated NBO Wiberg bond indices (which give more reliable information about the synchronicity of the reaction than the internuclear distances) are almost the same for these two contacts, that is, 0.38 and 0.39, respectively, and the synchronicity (S_y) calculated for the reaction of free CH_3CN using the formula reported previously[22,23] is 0.92 (for perfectly synchronous reactions, $S_y = 1$).

The coordination of CH_3CN results in a great increase of asynchronicity of the reaction mechanism which, nevertheless, remains to be concerted. The difference of the N(1)C(6) and C(2)O(5) distances rises upon coordination to 0.688 Å for **TS2** and to 0.763 Å for **TS3**, and the first contact is also longer than the second one. The corresponding Wiberg indices differ in ca. 0.35 (0.20 and 0.55 for **TS2** and 0.11 and 0.48 for **TS3**) and S_y is 0.69 for the reaction of **1** and 0.53 for that of **2**. The increase of the asynchronicity from **TS1** to **TS2** and **TS3** conceivably may be accounted for by the steric hindrances imposed by the Cl atoms, which elongate the C···N contact, and, probably, by the electronic influence of the metal in the complexes **1** and **2**. Indeed, the coordination of CH_3CN leads to a noticeable growth of the NBO atomic charge on the nitrile carbon atom from 0.29 to 0.48 in **1** and 0.53 in **2**[44] that facilitates the attack of the nucleophilic O-center of the nitrone molecule to the β-carbon atom of the coordinated nitrile and provides the shorter C···O contact in the transition state. At the same time, the negative NBO charge on the N atom of CH_3CN increases only insignificantly from −0.33 in CH_3CN to −0.36 and −0.34 in **1** and **2**, respectively. The relative contribution of the orbitals of the N and C nitrile atoms in the unoccupied π^*(CN) MOs is also similar for free and bound nitriles.

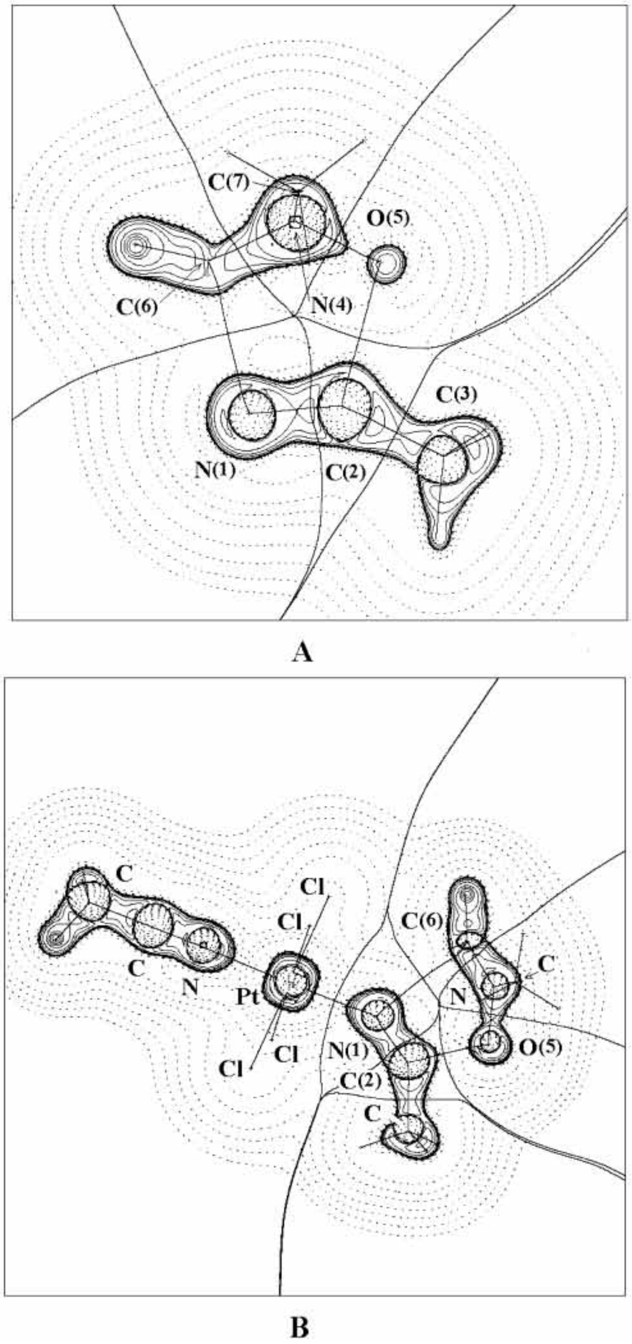

Figure 3. Contour line diagrams of the Laplacian distribution $\nabla^2\rho(\mathbf{r})$, bond paths and selected zero-flux surfaces in the plane formed by the N(1), C(2), O(5), and C(6) atoms for **TS1** (A) and **TS3** (B). Dashed lines indicate charge depletion ($\nabla^2\rho(\mathbf{r}) > 0$), solid lines indicate charge concentration ($\nabla^2\rho(\mathbf{r}) < 0$).

Another tool that can be useful for the investigation of the transition-state nature including the synchronicity is the topological analysis of the electron density distribution. This analysis was performed for two borderline cases, that is, **TS1** and **TS3**, and the contour line diagrams of the Laplacian distribution $\nabla^2\rho(\mathbf{r})$ are shown in Figure 3. The ring critical point was found for both structures suggesting that these TSs should be considered as cyclic ones and they correspond to the concerted cycloaddition. The bond critical points for the C(2)O(5) and N(1)C(6) contacts were found for **TS1** and **TS3**. The values of the electron density $\rho(\mathbf{r}_b)$ at both critical points are similar for

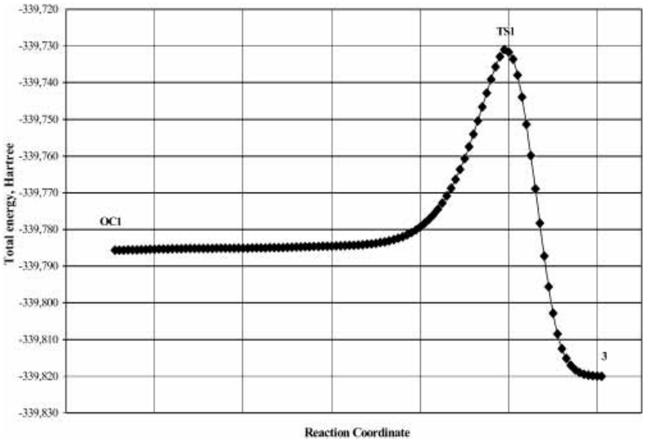

Figure 4. Calculated intrinsic reaction coordinate for the reaction of $H_2C{=}N(CH_3)O$ with CH_3CN.

TS1 (0.578 and 0.470 e Å^{-3} for C(2)O(5) and N(1)C(6), respectively) while, for **TS3**, $\rho(\mathbf{r}_b)$ at the C(2)O(5) contact [0.793 e Å^{-3}] is significantly higher than that at the N(1)C(6) contact [0.181 e Å^{-3}], in agreement with the above discussion. Correspondingly, a deformation of the electron charge distribution at the C(6) atom toward N(1) in **TS1** and at the C(2) atom to O(5) in both **TS1** and **TS3** is observed (Figure 3). The charge distribution at the C(6) atom in **TS3** remains without visible deformation. The energy density H_b at the CO bond critical point indicates some covalent contribution in the CO connection for **TS3** ($H_b = -0.282$ Hartree Å^{-3} being slightly negative) while for the CN contact in **TS3** and the CO and CN contacts in **TS1** H_b is close to zero demonstrating no covalent contribution.

The presence of the ring critical point, on one hand, and the small absolute value of $\rho(\mathbf{r}_b)$ for the N(1)C(6) contact, on the other hand, allow the characterization of **TS3** as a borderline case between the cyclic and the Michael-type structure (see below Stepwise Mechanism). Thus, the interaction of the nitrones with the Pt-bound nitriles also may be considered as intermediate between the "conventional" cycloaddition (reaction of the free nitrile) and the nucleophilic addition to the C(2) atom or even isolated into a separate class of the cycloaddition taking into account the opposite relationship between the activation energies and synchronicity of TS for free and ligated RCN (see below the section Influence of the Substituents). For the nucleophilic addition, the atomic charge on the C(2) atom is one of the factors determining the reactivity of the nitriles. As it was mentioned above, this charge is enhanced from CH_3CN to **1** and to **2** and may be considered as another reason of the activation of nitriles in the Pt-complexes toward the nitrone cycloaddition.

(ii) Mechanism. To investigate the concerted mechanism of the nitrone-to-nitrile cycloaddition in more detail, the calculations of the intrinsic reaction coordinate (IRC) starting from the found transition states have been carried out (see Computational Details) (Figure 4). The calculations indicate that the reactions proceed via the following pathway. On the first step, the approach of the reagents' molecules takes place to give the orientation complexes **OC1**−**OC3** (Figure 2). The nitrile fragments of these OCs are linear and the main bond lengths are similar to those for the starting compounds. The relative position of the $H_2C{=}N(CH_3){-}O$ and CH_3CN fragments in the OCs is characterized (at the B3LYP/6-31G* level) by the N(1)···C(6) and C(2)···O(5) distances of 4.802 and 3.358 Å (**OC1**), 3.643 and 2.759 Å (**OC2**), and 3.921 and 2.738 Å (**OC3**); by the N(1)C(6)N(4) and N(4)O(5)C(2) angles of 42.4 and 97.4° (**OC1**), 68.1 and 105.3° (**OC2**), and 67.3 and 113.4° (**OC3**); and by the N(4)C(6)N(1)C(2) and N(4)O(5)C(2)N(1) torsion angles of −79.1 and −32.1° (**OC1**), −54.1 and −2.8° (**OC2**), and −52.5 and −3.8° (**OC3**). The electronic energies of the OCs are by 6.15−10.26 kcal/mol lower than the sum of the energies of the reactants (Scheme 3a). However, the free Gibbs energy difference is positive for the formation of the orientation complexes ($\Delta G = 2.94$, 3.23, and 1.93 kcal/mol for **OC1**, **OC2**, and **OC3**, respectively, Scheme 3b) because of the strong decrease of the entropy from the reactants to OC ($\Delta S = 26.03{-}39.84$ cal/mol·K). The next phase on the reaction path is the transformation of the orientation complexes to the transition states as a result of the following approach of the initial molecules, bending of the nitrile fragment, formation of the new C···N and C···O contacts, and weakening of the N(1)−C(2) bond. On the final step, the TS transforms to the final products **3**−**5**.

(iii) Activation and Reaction Energies. The location of the transition states and the orientation complexes on the potential energy surface (PES) for the cycloaddition reaction allows the estimate of the electronic activation energies (E_a) for this process as well as the enthalpies and Gibbs free energies of activation ($\Delta H^‡$ and $\Delta G^‡$) (Table 2). The comparison of the activation parameters indicates that the E_a and $\Delta G^‡$ values relative to the reactants, that is, calculated as a difference of the total energies of the TS and the sum of the total energies of the reactants, decrease strongly from the reaction of free CH_3CN to that of complex **1** and further to that of **2** (Scheme 3). This correlates well with the experimentally observed enhancement of the reactivity of the nitriles along this sequence.[6,7] The activation energy for complex **2** has a negative value indicating that the **TS3** has lower electronic energy than the reactants' level. However, considering the formation of the orientation complex along the reaction path, the activation energy relative to **OC3** becomes positive (4.88 kcal/mol) (Scheme 3a). Such a situation was found, for instance, for the cycloaddition of azomethine ylides with acronitrile[35a] and of nitroethene with methyl vinyl ether in the presence of a Lewis acid.[45] Similarly, both free Gibbs energies of activation (relative to the reactants and to OC) are positive (8.04 and 6.11 kcal/mol, for the reaction of **2**) because of a strong decrease of the entropy from the reactants to OC and further to TS (Scheme 3b).

The reaction energies (ΔE) and enthalpies and free Gibbs energies (ΔH and ΔG) have negative values for all the processes (Table 2) demonstrating their exothermic character. Meanwhile, the absolute magnitudes of these parameters clearly increase from the reaction of free CH_3CN to that of complex **2** also in agreement with the experimentally found trend of the change of the reactivity in the row of the nitriles. Thus, the activation of the nitriles in the platinum complexes toward the nitrone cycloaddition and the enhancement of the reactivity from the Pt^{II} complex to that of Pt^{IV} can be interpreted in terms of both kinetic (the lowering of the activation parameters) and thermodynamic (growth of the negative values of the reaction energies) viewpoints.

The absolute values of the energies often depend strongly on the basis set and approach. With the aim to investigate how the change of the level of theory and basis set affects the energetic characteristics of the reaction, to evaluate the performance of the B3LYP/6-31G* calculations on the nitrone-to-nitrile cycloaddition, and to estimate the reliable absolute values of the activation and reaction energies, the structures of the reactants, products, transition states, and orientation complexes for the reaction of free CH_3CN with $H_2C{=}N(CH_3)O$ have been calculated at different levels including such high-correlated

SCHEME 3: Energy Profile of Reactions of CH_3CN, 1, and 2 with $H_2C{=}N(CH_3)O$ in Terms of ΔE (A) and ΔG (B) Values

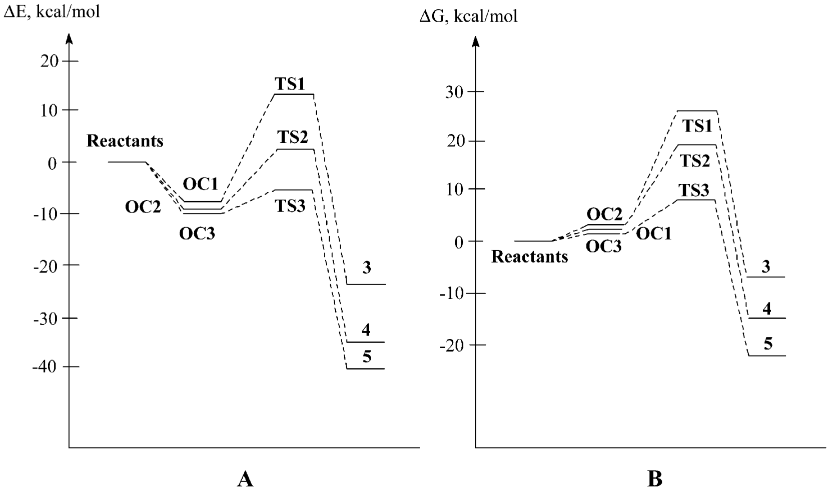

TABLE 2: Energetic Characteristics (in kcal/mol) of the Cycloaddition Reactions of *N*-Methyl Nitrone to Free CH_3CN and to the Complexes 1 and 2 Relative to the Reactants (Plain Text) and to the Orientation Complex (Bold Text) for the B3LYP/6-31G* Level[a]

dipolarophile	E_a	$\Delta H^{\ddagger}$	$\Delta G^{\ddagger}$	ΔE	ΔH	ΔG
CH_3CN	13.99 (15.73)	14.90	27.65	−23.78 (−19.91)	−21.14	−7.60
	15.92	[17.76][c]	[30.47][c]	*−21.85*	[−20.56][c]	[−7.09][c]
	[16.86][b]	**19.72**	**24.71**	[−23.13][b]		
	[16.89 (18.57)][c]			[−23.11 (−19.36)][c]		
	20.14 (21.07)					
1	3.02 (4.53)	3.29	19.58	−35.19 (−31.13)	−32.83	−15.31
	5.68	**11.94**	**16.36**	*−32.54*		
	[6.52][b]			[−30.73][b]		
	12.46 (13.18)					
2	−5.38 (−3.99)	−3.93	8.04	−40.69 (-36.27)	−37.05	−22.17
	−3.59	**4.93**	**6.11**	*−38.90*		
	[0.10][b]			[−36.01][b]		
	4.88 (5.38)					

[a] Zero-point energy-corrected values in parentheses, the BSSE-corrected values are given in italics, the energies corrected on the solvent effect are given in square brackets. [b] Single-point CPCM-calculations based on the gas-phase equilibrium geometry. [c] Full geometry optimization at the CPCM-B3LYP/6-31G* level.

methods as MP4(SDTQ), CCSD(T), and CBS-Q. The activation parameters and the reaction energies were calculated for this process at all these approaches.

The inspection of the *activation energies relative to the reactants* in Table 3 shows, first, that the Hartree−Fock E_a values are significantly higher in comparison with the correlated methods indicating the great importance of the electron correlation effects for the estimate of E_a, $\Delta H^{\ddagger}$, and $\Delta G^{\ddagger}$ of the nitrone-to-nitrile cycloaddition. Second, the change of the geometry does not affect significantly the energetic characteristics. Indeed, the difference of the electronic activation energies for the MP2//HF/6-31+G** and MP2//MP2/6-31+G**, MP4(SDTQ)//MP2/6-31G* and MP4(SDTQ)//B3LYP/6-31G*, and CCSD(T)//MP2/6-31G* and CCSD(T)//B3LYP/6-31G* levels is only 1.26, 0.44, and 0.23 kcal/mol, respectively. Third, the extension of the basis set results in the increase of the activation energies that was found for all levels, especially for B3LYP (the CBS-Q method uses large basis sets, up to 6-311+G(2df) on the first-row atoms).

The E_a, $\Delta H^{\ddagger}$, and $\Delta G^{\ddagger}$ values are weakly sensitive to a change of the correlated methods, a situation quite different from that found, for example, for the cycloaddition of diazomethane to ethylene[32e] or fulminic acid to acetylene[32d] where a 2- or even 3-fold variation of E_a was detected, depending on the approximation. Indeed, our calculations indicate that the B3LYP electronic activation energies are only by 1.09−3.95 kcal/mol higher in comparison with the MP2 values obtained at the same basis set and the $\Delta\Delta G^{\ddagger}$ difference is 0.87−3.70 kcal/mol. The extension of the level within the Møller−Plesset method, that is, from MP2 to MP3, leads to the increase of E_a by 4.76 kcal/mol. However, a further improvement of the approach up to MP4(SDTQ) level results again in the decrease of E_a to 12.13−12.57 kcal/mol that is very close to the values obtained at the second order of the Møller−Plesset theory. The use of the coupled-cluster method with singles, doubles, and noniterative estimate of triple excitations CCSD(T), on the basis of the MP2/6-31G* and B3LYP/6-31G* geometries, gives slightly higher magnitudes for the activation parameters (by 1.61−1.82 kcal/mol in comparison with MP4(SDTQ)) whereas the CBS-Q calculations lead to a slightly lower barrier.

Similar trends were obtained for the activation parameters *relative to the orientation complex*, which have, apparently, higher values for E_a and $\Delta H^{\ddagger}$ in comparison with the energies relative to the reactants. However, the Gibbs free energy difference of activation is lower for the former case than for the latter one because the entropy decrease from the reactants to the OC is significantly higher (by 4.70−12.97 cal/mol·K) than that from OC to TS. The energetic characteristics for the conversion of the reactants to the orientation complex weakly depend on the basis set and level of theory (including HF) with maximum deviation of 3.55 kcal/mol for ΔE, 4.17 kcal/mol for ΔH, and 4.12 kcal/mol for ΔG.

TABLE 3: Electronic Activation Energies (E_a), Enthalpies ($\Delta H^{\ddagger}$), and Free Gibbs Energies ($\Delta G^{\ddagger}$) of Activation (in kcal/mol) for the Cycloaddition Reaction of *N*-Methyl Nitrone ($H_2C{=}N(CH_3)O$) to Acetonitrile (CH_3CN) Relative to the Reactants (Plain Text) and to the Orientation Complex (Bold Text)[a]

method and basis set	E_a	$\Delta H^{\ddagger}$	$\Delta G^{\ddagger}$
HF//HF/6-31G	25.40 (27.46)	26.54	39.53
	26.91	**28.94**	**34.05**
	32.53 (33.75)		
HF//HF/6-31G*	28.71 (30.67)	29.78	42.73
	30.08	**34.42**	**39.76**
	34.72 (35.92)		
HF//HF/6-31+G**	31.14 (33.01)	32.13	45.04
	31.43	**36.29**	**41.52**
	36.65 (37.76)		
HF/6-311++G**//HF/6-31+G**	31.81		
	32.02		
	37.33		
MP2//HF/6-31+G**	11.23		
	12.65		
	18.26		
MP2//MP2/6-31G*	12.29 (14.64)	13.62	26.78
	15.20	**19.86**	**24.86**
	19.84 (21.34)		
MP2//MP2/6-31+G**	12.49 (14.85)	13.80	27.01
	14.72	**20.36**	**25.65**
	20.27 (21.97)		
MP2/6-311++G**//MP2/6-31+G**	13.08		
	15.05		
	20.64		
B3LYP//B3LYP/6-31G	12.17 (13.95)	13.11	25.91
	14.36	**18.75**	**23.22**
	19.16 (20.04)		
B3LYP//B3LYP/6-31G*	13.99 (15.73)	14.90	27.65
	15.92	**19.72**	**24.71**
	20.14 (21.07)		
B3LYP//B3LYP/6-31+G**	17.08 (18.80)	17.97	30.71
	17.14	**21.53**	**26.84**
	21.92 (22.95)		
B3LYP/6-311++G**// B3LYP/6-31+G**	18.24		
	18.30		
	23.02		
MP3//MP2/6-31G*	17.05		
	19.82		
	24.34		
MP4(SDTQ)//MP2/6-31G*	12.57		
	15.61		
	19.91		
MP4(SDTQ)//B3LYP/6-31G*	12.13		
	14.78		
	19.34		
CCSD(T)//MP2/6-31G*	14.18		
	17.17		
	21.50		
CCSD(T)//B3LYP/6-31G*	13.95		
	16.55		
	21.20		
CBS-Q	11.50	10.67	23.43
	17.01	**15.56**	**21.24**

[a] Zero-point energy-corrected values in parentheses, the BSSE-corrected values are given in italics.

TABLE 4: Electronic Reaction Energies (ΔE), Enthalpies (ΔH), and Free Gibbs Energies (ΔG) of the Reaction (in kcal/mol) for the Cycloaddition of *N*-Methyl Nitrone ($H_2C{=}N(CH_3)O$) to Acetonitrile (CH_3CN) Relative to the Reactants[a]

level and basis set	ΔE	ΔH	ΔG
HF//HF/6-31G	−15.71 (−11.40)	−12.61	0.82
	−14.19		
HF//HF/6-31G*	−27.56 (−23.00)	−24.28	−10.62
	−26.18		
HF//HF/6-31+G**	−23.50 (−18.99)	−20.27	−6.63
	−23.22		
HF/6-311++G**//HF/ 6-31+G**	−22.35		
	−22.15		
MP2//HF/6-31+G**	−21.79		
	−20.37		
MP2//MP2/6-31G*	−22.96 (−18.37)	−19.78	−5.81
	−20.06		
MP2//MP2/6-31+G**	−20.15 (−15.60)	−17.03	−3.00
	−17.92		
MP2/6-311++G**//MP2/ 6-31+G**	−20.26		
	−18.29		
B3LYP//B3LYP/6-31G	−14.78 (−11.26)	−12.43	1.01
	−12.59		
B3LYP//B3LYP/6-31G*	−23.78 (−19.91)	−21.14	−7.60
	−21.85		
B3LYP//B3LYP/6-31+G**	−18.45 (−14.61)	−15.85	−2.29
	−18.39		
B3LYP/6-311++G**// B3LYP/6-31+G**	−15.22		
	−15.15		
MP3//MP2/6-31G*	−30.12		
	−27.35		
MP4(SDTQ)//MP2/6-31G*	−22.67		
	−19.63		
MP4(SDTQ)//B3LYP/6-31G*	−22.81		
	−20.16		
CCSD(T)//MP2/6-31G*	−24.86		
	−21.87		
CCSD(T)//B3LYP/6-31G*	−24.66		
	−22.06		
CBS-Q	−19.59	−20.80	−7.34

[a] Zero-point Energy Corrected Values in Parentheses, the BSSE-corrected Values Are Given in Italics.

Another effect that often affects noticeably the calculated energies is the basis set superposition error (BSSE). Indeed, our calculations with the counterpoise estimates of BSSE indicate that the BSSE correction increases the activation barrier by 0.06−3.04 kcal/mol, and such an increase is found mainly for the relatively small basis sets while for the extended ones, for example, 6-311++G**, the difference is smaller (up to 0.06 kcal/mol for B3LYP/6-31+G** and B3LYP/6-311++G**). Thus, the BSSE corrected activation energies are less sensitive to the change of the basis set as well as of the method, for example, the energies calculated at B3LYP/6-31G*, MP2/6-31G*, MP4(SDTQ)//MP2/6-31G*, and MP4(SDTQ)//B3LYP/6-31G* levels vary within the range of 1.14 kcal/mol, although the MP3 and CCSD(T) approaches also give slightly higher estimates for E_a (19.82, 17.17, and 16.55 kcal/ mol).

Unfortunately, there are no experimental data about the activation energies for a cycloaddition to simple alkylnitriles. Meanwhile, it was shown[17] that the Complete Basis Set schemes of Petersson and co-wokers, for instance, the CBS-Q method[17f] used by us, allow to get very accurate absolute energies which are often very close to the experimental ones. Hence, the CBS-Q energies may be taken as reference values for comparison with those obtained by other methods. Such comparison shows that the results of the calculations at the B3LYP/6-31G* level (one of the least expensive approaches among the correlated ones used by us) agree well with those computed using the higher correlated methods, and this functional may be recommended to be applied for the calculations of the nitrone-to-nitrile cycloaddition.

The *reaction energies* (Table 4) appear to be rather sensitive to a change of the basis set, especially to the insertion of the polarization functions. Indeed, changing from the 6-31G to the 6-31G* basis sets results into a 2-fold increase of the absolute magnitude of the reaction energy. A further extension of the basis set leads to some decrease of $|\Delta E|$. Meanwhile, the correlated methods, including the high-level ones, give rather similar values for the reaction energy for the same basis set (e.g., in the range −22.67 to −24.86 kcal/mol for 6-31G*) except the MP3 approach. The Hartree−Fock method also only slightly overestimates the reaction energy in comparison with the correlated levels. The CDS-Q calculations result in ΔE and ΔG values of −19.59 and −7.34 kcal/mol, respectively, which are close to those obtained at the B3LYP/6-31G* level (−23.78 and −7.60 kcal/mol, respectively). The BSSE correction reduces the values of $|\Delta E|$ by 0.06−3.04 kcal/mol, and this lowering is also not significant for the extended basis sets, especially for B3LYP.

(iv) Solvent Effects. The experimentally studied reactions of the cycloaddition of nitrones to nitriles have proceeded in CH_2Cl_2 solution.[6,7] To take into account the influence of the solvent on the energetic characteristics of the reactions, the calculations of the activation parameters and the reaction energies for the interaction of $H_2C{=}N(CH_3)O$ with CH_3CN, **1** and **2**, have been performed using the self-consistent reaction field method based on the CPCM model. For the cycloaddition to free nitrile, the geometries of the molecules have been fully optimized at the CPCM-B3LYP/6-31G* level. As a result, the transition state **TS1** becomes slightly more asynchronous, for example, the difference of the N(1)C(6) and C(2)O(5) internuclear distances increases from 0.131 Å for gas phase to 0.167 Å for solution and the difference of the Wiberg indices rises from 0.01 to 0.03. Other bond lengths in **TS1** as well as those in $H_2C{=}N(CH_3)O$, CH_3CN, and **3** change only insignificantly upon inclusion of the solvent effect. Meanwhile, the CPCM-geometry optimization almost does not affect the E_a and ΔE values in comparison with the single-point CPCM-calculations based on the B3LYP/6-31G* gas-phase geometry (Table 2). Therefore, for the reactions of **1** and **2**, only the single-point calculation of the solvent effect was carried out.

The effect of solvation (i) increases the activation barriers (by 2.87−5.48 kcal/mol) and (ii) decreases the negative values of the reaction energies (by 0.65−4.68 kcal/mol, Table 2). This situation is due to a higher stabilization of the reactants' level in comparison with the TSs or the final products **3**−**5** upon going from the gas phase to solution that is accounted for by the strongly polar character of the reactants' molecules. The total solvent effect within the CPCM model (in terms of ΔG of solvation, ΔG_{solv}) can be split into two contributions, the electrostatic component (EL) and the nonelectrostatic one (non-EL), the latter including the cavitation, dispersion, and repulsion terms. The analysis of the contribution of these components into ΔG_{solv} (Table 5) indicates that the EL term is strongly negative for each particular structure. The non-EL component is negative only for the nitrone, **TS1**, and **3** (because of a relatively high dispersion component that is negative), whereas for the initial Pt-complexes **1** and **2**, corresponding TSs (**TS2** and **TS3**), and products (**4** and **5**), the non-EL component is positive (predominance of the positive cavitation term). Nevertheless, the total solvent effect is negative for all species.

The calculations of the *relative* solvent effect, that is, that of TSs [$\Delta\Delta G^{\ddagger}_{solv} = \Delta G_{solv}(\mathrm{TS}) - \Sigma\Delta G_{solv}$ (reactants)] and the final complexes [$\Delta\Delta G_{solv} = \Delta G_{solv}$ (product) $- \Sigma\Delta G_{solv}$ (reactants)] relative to the reactants, indicate that the electrostatic term ($\Delta EL^{\ddagger}$ and ΔEL) plays the main role in the increase of E_a and decrease of $|\Delta E|$ from the gas phase to the solution while the Δnon-EL‡ and Δnon-EL components are comparatively small except the Δnon-EL for the reaction of free CH_3CN (Table 5). Both $\Delta\Delta G^{\ddagger}_{solv}$ and $\Delta\Delta G_{solv}$ effects increase from the reaction of CH_3CN to that of **2**, determining the growing difference between the gas phase and CPCM-energies along this sequence. Meanwhile, the general trend of the change of E_a and ΔE in solution from the free nitrile to the complexes of Pt^{II} and further of Pt^{IV} remains the same as that for the gas phase, that is, a significant reduction of the E_a, and increase of the $|\Delta E|$ values take place.

TABLE 5: Absolute (ΔG_{solv}) and Relative to the Reactants ($\Delta\Delta G_{solv}{}^{\ddagger}$ and $\Delta\Delta G_{solv}$) Solvent Effects (in kcal/mol)[a]

Structure	EL	Non-EL	ΔG_{solv}
$H_2C{=}N(CH_3)O$	−3.25	−0.74	−3.99
CH_3CN	−2.88	−0.04	−2.92
1	−9.90	+3.23	−6.68
2	−11.32	+5.14	−6.19
TS1	−2.92	−1.13	−4.05
TS2	−9.57	+2.36	−7.21
TS3	−9.92	+5.21	−4.70
3	−3.52	−2.75	−6.27
4	−8.55	+2.33	−6.23
5	−8.90	+3.40	−5.51

Dipolarophile	$\Delta EL^{\ddagger}$	ΔNon-EL‡	$\Delta\Delta G_{solv}{}^{\ddagger}$	ΔEL	ΔNon-EL	$\Delta\Delta G_{solv}$
CH_3CN	+3.21	−0.35	+2.86	+2.61	−1.97	+0.64
1	+3.58	−0.13	+3.45	+4.59	−0.17	+4.44
2	+4.65	+0.81	+5.46	+5.68	−1.00	+4.68

[a] Electrostatic and non-electrostatic components are denoted EL and non-EL, respectively.

(v) Influence of the Substituents. The *N*-methyl nitrone $H_2C{=}N(CH_3)O$ and acetonitrile CH_3CN have been used for the calculations as the simplest models, the former being a hypothetical compound, but experimental data on the cycloaddition to nitriles are available for C-substituted nitrones $H(R)C{=}N(R')O$ [$R = {}^{t}Bu$, Ph, *o*-C_6H_4OH, *p*-C_6H_4-X ($X = CH_3$, OCH_3, NO_2); $R' = CH_3$, CH_2Ph] and for the Pt-bound nitriles CH_3CN and PhCN.[6,7] Obviously, the nature of the substituents should affect the reactivity for both the nitrone and the nitrile. Hence, to study the substituent effect, an additional theoretical investigation of the reactions of $H(CH_3)C{=}N(CH_3)O$ (**6**) and $H(p\text{-}C_6H_4CH_3)C{=}N(CH_3)O$ (**7**) with CH_3CN, $H(p\text{-}C_6H_4OCH_3)C{=}N(CH_3)O$ (**8**) with CH_3CN and PhCN, and $H_2C{=}N(CH_3)O$ with PhCN, to give the products **9**−**13** (Figure 2), has been carried out, including the location of the final product and transition states and the estimate of the main energetic characteristics of the reactions.

The consideration of the frontier MO composition of the nitrones indicates that the HOMO energy increases along the row $H_2C{=}N(CH_3)O$−**6**−**7**−**8** (Scheme 2). The LUMO energy of **6** is higher but that of the phenyl-substituted nitrones is lower than that for the *N*-methyl nitrone demonstrating a narrower HOMO−LUMO gap for **7** and **8** in agreement with the data reported previously,[31c] although the LUMO energy of **8** is slightly (by 0.17 eV) higher than that of **7**. Thus, the frontier molecular orbital theory arguments suggest that the enhancement of the reactivity of the phenyl-substituted nitrones is due to the decrease of both $\mathrm{HOMO_{nitrone-}LUMO_{nitrile}}$ and $\mathrm{LUMO_{nitrone-}HOMO_{nitrile}}$ gaps.

However, a more detailed theoretical study of these reactions predicts the opposite trend of the reactivity change. The calculated activation barriers for the reactions of **6**, **7**, or **8** with CH_3CN (**TS4**, **TS5**, and **TS6** are corresponding transition states) are noticeably (by 2.12, 6.60, or 6.44 kcal/mol, respectively) higher than that for the reaction of $H_2C{=}N(CH_3)O$ with acetonitrile (Table 6), which is probably due to the lower orbital coefficients at the reacting centers, especially at the C(6) atom, and to a possible steric hindrance imposed by the phenyl ring. Indeed, the replacement of the hydrogen by the methyl, *p*-methyl-, or *p*-metoxy-phenyl group results in the increase of the asynchronicity of the respective transition state, for example,

TABLE 6: Energetic Characteristics (in kcal/mol) of the Cycloaddition of the Substituted Nitrones ($H(R')C{=}N(CH_3)O$) to Free Nitriles (RCN) Relative to the Reactants for the B3LYP/6-31G* Level[a]

R	R′	E_a	$\Delta H^{\ddagger}$	$\Delta G^{\ddagger}$	ΔE	ΔH	ΔG
CH_3	H	13.99 (15.73)	14.90	27.65	−23.78 (−19.91)	−21.14	−7.60
CH_3	CH_3	16.11 (17.83)	16.89	30.30	−21.28 (−17.50)	−16.89	−4.73
CH_3	*p*-$C_6H_4CH_3$	20.59 (21.75)	21.07	34.08	−14.46 (−11.32)	−12.93	+2.12
CH_3	*p*-$C_6H_4OCH_3$	20.43 (21.60)	20.94	33.79	−14.14 (−11.01)	−12.05	+1.02
Ph	H	12.96 (14.49)	13.87	26.97	−25.13 (−21.45)	−22.48	−8.37
Ph	*p*-$C_6H_4OCH_3$	19.28 (20.26)	19.84	33.15	−15.38 (−12.50)	−13.27	+0.41

[a] Zero-point energy-corrected values in parentheses.

the difference of the N(1)C(6) and C(2)O(5) internuclear distances rises from 0.131 Å for **TS1** to 0.162, 0.223, and 0.234 Å for **TS4**, **TS5**, and **TS6**, respectively, with the CN contact longer than the CO one. The difference of the Wiberg indices for these contacts are 0.03, 0.07, and 0.07 for these TSs. The $\Delta G^{\ddagger}$ increases from 27.65 kcal/mol for $H_2C{=}N(CH_3)O + CH_3CN$ to 30.30, 34.08, and 33.79 kcal/mol for **6**, **7**, and **8** + CH_3CN, respectively. The predicted decrease of the reactivity from the C-alkyl to the C-aryl substituted nitrones is in agreement with the experimental observations.[6,7,46] The reactivity of **7** and **8** should be similar and the latter appears to be slightly more reactive than the former.

The reaction energies increase along the row $H_2C{=}N(CH_3)O$−**6**−**8**−**7** and the ΔG value becomes positive for the C-phenylnitrones (Table 6). Thus, the high magnitudes of $\Delta G^{\ddagger}$ and positive ΔG of reactions **7** and **8** explain the experimental data, suggesting that these nitrones do not react with the uncoordinated acetonitrile even under harsh conditions.[6]

The replacement of methyl by phenyl in the nitrile molecule results, as expected, in some decrease of the activation barrier and increase of the negative reaction energies, correlating with the narrower HOMO−LUMO gap for PhCN than for CH_3CN. The corresponding transition state **TS7** is less asynchronous than **TS1** with the N(1)C(6) and C(2)O(5) distance difference of 0.081 Å and with equal Wiberg indices. Finally, for the reaction of **7** with PhCN, two opposite effects of the substituents take place. As a result, the activation barrier for this process is also significantly higher (by ca. 6 kcal/mol) than for the reaction of $H_2C{=}N(CH_3)O$ with PhCN but by ca. 1 kcal/mol lower than for the reaction of **7** with CH_3CN. The calculated $\Delta H^{\ddagger}$ value is consistent with the experimental parameter found for the reaction of a cyclic nitrone with benzonitrile (20.1 kcal/mol).[47]

For the uncoordinated reagents, there is a rather good correlation between the synchronicity of the TS (in terms of the bond lengths or Wiberg indices differences which are more sensitive than the values of S_y) and the activation barrier (Figure 5), an increase of the former corresponding to a growth of the latter and the reaction should proceed easier via formation of the more synchronous TS. For the reaction of free nitriles, this trend may be accounted for by the better overlap of the interacting HOMO and LUMO of the reactants for the synchronous TS than for the asynchronous one, leading to the lowering of the relative energy of the former TS. However, for the reaction of the nitrile complexes **1** and **2**, the activation barriers are significantly lower despite the higher asynchronicity of **TS2** and **TS3** in comparison with **TS1**. In the complexes, there is another factor to be considered, that is, the activation of the β-carbon atom of the bound nitrile toward the nucleophilic addition (almost a 2-fold rising of the NBO effective charges on this atom from free to ligated CH_3CN was found[44] with nearly no charge alteration on the N atom). This activation facilitates the one-end addition of the nitrones to nitriles by the O atom. These two factors, that is, the maximum HOMO−LUMO overlap and the activation of the β-C atom, are opposite and, for the bound nitriles, the latter predominates over the former. Thus, the cycloadditions of the nitrones to free or bound nitriles indeed can be assigned to two types of mechanism *within the concerted pathway* (see above).

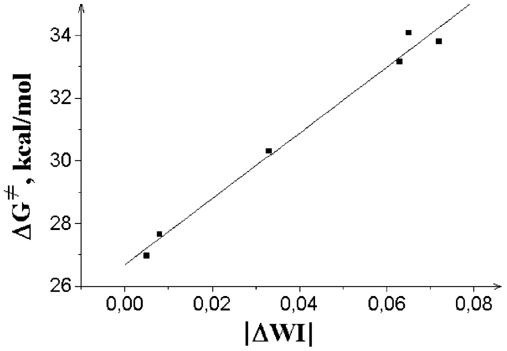

Figure 5. Dependence of $\Delta G^{\ddagger}$ on the difference of the Wiberg indices of the C(2)O(5) and N(1)C(6) bonds (ΔWI) for the reactions of uncoordinated nitriles RCN (R = H, Ph) with nitrones $H(R')C{=}N(CH_3)O$ (R′ = H, CH_3, *p*-$C_6H_4CH_3$, *p*-$C_6H_4OCH_3$) for B3LYP/6-31G* level.

Stepwise Mechanism. Another plausible pathway for the cycoaddition reactions, originally proposed by Firestone,[40] is the stepwise mechanism involving the initial (nucleophilic) addition of the dipole molecule to the dipolarophile by one center to give a Michael-type intermediate or transition state, followed by the cycle closure to form the final cycloaddition product. Although this mechanism is not supported by the majority of authors, it cannot be excluded especially for the reactions of the nitriles coordinated to a transition metal. Therefore, we investigated the possibility of the stepwise mechanism for the reaction of free CH_3CN and the complex **2** as two borderline cases, by a detailed search of the potential energy surface and the location of possible stepwise intermediates and TSs in different spin states. For the $H_2CN(CH_3)O + CH_3CN$ system, two types of the stepwise addition product were examined, that is, $NC(CH_3)ON(CH_3)CH_2$ (type **A**) and $N(CCH_3)$-$CH_2N(CH_3)O$ (type **B**) bearing either the C(2)O(5) or the N(1)C(6) bond between the reactant molecules. For both of these types, various starting conformations of the $H_2CN(CH_3)O$ molecule relative to the nitrile have been used. As a result, 2 singlet dipolar, 16 triplet biradical (B3LYP/6-31G*), and no singlet biradical (GVB−PP(1)/6-31G*) intermediates or transition states—which, in principle, could be involved in the stepwise mechanism—were found. However, the energies of all these structures are higher, by 21.1−49.3 kcal/mol, than those of the **TS1**, that is, the transition state for the concerted mechanism.

As it was found,[44] the coordination of CH_3CN to the metal leads to an increase of the electrophilicity of its β-carbon atom that might result in favor of the stepwise mechanism via the initial nucleophilic attack at that atom by the oxygen of the nitrone. However, for the $H_2C{=}N(CH_3)O$ + **2** system, no singlet dipolar or triplet biradical structures of the “pure” Michael-type [i.e., that bearing only the C(2)O(5) but no N(1)C(6) bond] at the B3LYP/6-31G* level and no singlet biradical structures at the GVB−PP(1)/6-31G* level have been found. All attempts to locate the intermediates and TSs of such type resulted in the removing of the reactants' molecules from each other or the formation of the singlet dipolar final products or the transition states corresponding to the concerted mechanism. Thus, the calculations do not support the stepwise mechanism of the nitrone-to-nitrile cycloaddition either for free CH_3CN or for the Pt-bound nitriles.

4. Final Remarks

The experimentally observed[6,7] activation of nitriles in platinum complexes toward cycloaddition of nitrones and the enhancement of their reactivity from the complexes of Pt^{II} to those of Pt^{IV} can be interpreted in terms of both kinetic (dramatic decrease of the activation barrier by ca. 17−19 kcal/mol) and thermodynamic (growth of the absolute values of the reaction energies) viewpoints. For the related Lewis acid catalyzed normal electron-demand reaction of nitrone ($H_2C{=}NHO$) with acrolein $CH_2{=}CHCHO$, a significantly smaller decrease of the activation parameters (by 1.0−12.5 kcal/mol) was found by Tanaka and Kanemasa.[33b] For the inverse electron-demand BH_3- or $AlMe_3$-catalyzed cycloaddition of nitrones to olefins, the acceleration effect was predicted to be smaller (3.0−4.2 kcal/mol) or even switched to inhibition of the reaction.[33a,b]

Our calculations show that the cycloaddition of nitrones to nitriles is mainly determined by the $HOMO_{nitrone}$−$LUMO_{nitrile}$ type of interaction (the normal electron-demand process) even for the acetonitrile with the electron-donor methyl group. At the same time, for the alkenes as dipolarophiles, the predominance of the type of the HOMO−LUMO interaction depends more crucially on the nature of the substituent than in the nitriles. For electron-donor groups at the alkene, like methoxy or even methyl, the $HOMO_{alkene}$−$LUMO_{nitrone}$ type prevails[31c,33a] while for the electron-withdrawing groups, the normal electron-demand process is followed.[31c,33c] The FMO consideration suggests that promotion of the nitrone-to-nitrile cycloaddition can be achieved by the selective Lewis acid coordination *to nitrile* rather than to nitrone. Indeed, the ligation of the nitriles and increase of the metal oxidation state lead to lowering of the virtual π^*(CN) MOs energy, thus providing the activation effect. However, for the cycloaddition to alkenes, the promotion may be reached by Lewis acid ligation either to alkene or to nitrone, depending on the substituents.

Both general mechanisms of cycloaddition, that is, concerted and stepwise, have been investigated in detail, and the calculations support the former pathway via formation of one five-membered transition state. The reactions of the nitrones with uncoordinated and ligated nitriles may be assigned to two types of cycloaddition *within the concerted mechanism*. For the reactions of free nitriles, the cycloaddition is nearly *synchronous*, and the reactivity of the RCN (in terms of the activation barriers) correlates with the synchronicity of the process. For the Pt-bound nitriles, the cycloaddition is *asynchronous* and the respective TSs are characterized as a borderline case between the cyclic and the Michael-type structure. The interaction of the nitrones with the complexes **1** and **2** may be considered as intermediate between the "conventional" synchronous cycloaddition (reaction of the free nitriles) and the nucleophilic addition to the β-C atom. Thus, the increase of the effective atomic charge on this atom upon coordination is another driving force of the nitrile activation by the metal centers in the complexes.

The concerted mechanism was also found to be common for the related reactions of the nitrones with alkenes and alkynes.[32k,33e,f] The synchronicity of these processes depends on the nature of substituents, on the regioisomeric pathway, and on the presence of a Lewis acid as a catalyst. For instance, the cycloaddition of C-methyl-*N*-methylnitrone ($H(CH_3)C{=}N(CH_3)O$) to methyl vinyl ether ($H_2C{=}CHOCH_3$) along the *meta* pathways is almost synchronous (the difference of the Wiberg bond indices of two new contacts in the TSs is 0.01−0.04) whereas for the *ortho* pathways as well as for the reactions of the nitrones with methyl propiolate ($HC{\equiv}CC(O)OCH_3$) and acrylonitrile ($H_2C{=}CHCN$) there is a noticeable degree of asynchronicity.[33a,c] It is interesting that the cycloaddition of nitrones to nonsubstituted ethylene and acetylene[23] has the same synchronicity as the reaction with free acetonitrile ($S_y = 0.92$ for all processes) despite the change of the nature of one of the reacting atoms toward the dipolarophile molecule. It also seems that the increase of the asynchronicity as a result of the Lewis acid coordination is the general rule for the reactions of the nitrone cycloaddition.[33a] In the interaction of the nitrone with acrolein bound with BF_3, the stepwise mechanism was even more probable than the concerted one.[33b] However, these results have to be taken cautiously because the calculations have been performed at the HF level without considering the electron correlation effects.

The influence of the nature of the substituents in the nitrone and nitrile molecules on the reactivity has also been investigated in the present work. The calculations suggest that the C-substituted nitrones are significantly less reactive than the nonsubstituted $H_2C{=}N(CH_3)O$ one, and the activation barriers of the aryl-substituted nitrones are higher than those of the C-alkyl nitrones. However, benzonitrile exhibits a higher reactivity than acetonitrile. The influence of the substituents at the nitrone on the reactivity is much higher than that found for the cycloaddition of nitrile oxides ($RC{\equiv}NO$) to cyanoacetylene ($HC{\equiv}CCN$): the replacement of the hydrogen atom by the mesityl group in $RC{\equiv}NO$ (R = H or mesityl) does not affect the activation energy in gas phase.[32c]

The activation parameters and reaction energies have been calculated by us at different basis sets and levels of theory, that is, HF, B3LYP, MP2, MP3, MP4(SDTQ), CCSD(T), and CBS-Q. The activation energies are weakly sensitive to a change of the method (except the HF one). This situation is quite different from that found for the cycloaddition of diazomethane to ethylene[32e] or of fulminic acid to acetylene[32d] where a 2- or even 3-fold variation of E_a was detected, depending on the approximation. Our results of the calculations at the B3LYP/6-31G* level (one of the least expensive approaches among the correlated ones used by us) agree well with those computed at the higher correlated methods. Thus, this functional may be recommended to be applied for the calculations of the nitrone-to-nitriles cycloaddition reactions.

Acknowledgment. M. L. K. (grant BPD16369/98//BPD/5558/2001) is very much obliged to the PRAXIS XXI and POCTI programs (Portugal) for the fellowships. A. J. L. P. and V. Yu. K. are grateful to the FCT (Foundation for Science and Technology) (Portugal) and the PRAXIS XXI and POCTI programs (project QUI/43415/2001, FEDER supported) for financial support of these studies.

References and Notes

(1) Padwa, A. *1,3-Dipolar Cycloaddition Chemistry*; Wiley: New York, 1984.

(2) Kukushkin, V. Yu.; Pombeiro, A. J. L. *Chem. Rev.* **2002**, *102*, 1771.

(3) Gothelf, K. V.; Jørgensen, K. A. *Chem. Rev*. **1998**, *98*, 863.

(4) Fukui, K. *Theory of Orientation and Stereoselection*; Springer-Verlag: Berlin, 1975.

(5) Gothelf, K. V.; Jørgensen, K. A. *Chem. Commun*. **2000**, 1449.

(6) Wagner, G.; Pombeiro, A. J. L.; Kukushkin, V. Yu. *J. Am. Chem. Soc*. **2000**, *122*, 3106.

(7) Wagner, G.; Haukka, M.; Fraústo da Silva, J. J. R.; Pombeiro, A. J. L.; Kukushkin, V. Yu. *Inorg. Chem*. **2001**, *40*, 264.

(8) Bokach, N. A.; Khripoun, A. V.; Kukushkin, V. Yu.; Haukka, M.; Pombeiro, A. J. L. *Inorg. Chem*. **2003**, *42*, 896.

(9) Frisch, M. J.; Trucks, G. W.; Schlegel, H. B.; Scuseria, G. E.; Robb, M. A.; Cheeseman, J. R.; Zakrzewski, V. G.; Montgomery, J. A., Jr.; Stratmann, R. E.; Burant, J. C.; Dapprich, S.; Millam, J. M.; Daniels, A. D.; Kudin, K. N.; Strain, M. C.; Farkas, O.; Tomasi, J.; Barone, V.; Cossi, M.; Cammi, R.; Mennucci, B.; Pomelli, C.; Adamo, C.; Clifford, S.; Ochterski, J.; Peterson, G. A.; Ayala, P. Y.; Cui, Q.; Morokuma, K.; Malick, D. K.; Rabuck, A. D.; Raghavachari, K.; Foresman, J. B.; Cioslowski, J.; Ortiz, J. V.; Baboul, A. G.; Stefanov, B. B.; Liu, G.; Liashenko, A.; Piskorz, P.; Komaromi, I.; Gomperts, R.; Martin, R. L.; Fox, D. J.; Keith, T.; Al-Laham, M. A.; Peng, C. Y.; Nanayakkara, A.; Challacombe, M.; Gill, P. M. W.; Johnson, B.; Chen, W.; Wong, M. W.; Andres, J. L.; Gonzalez, C.; Head-Gordon, M.; Replogle, E. S.; Pople, J. A. *Gaussian 98*, revision A.9; Gaussian, Inc.: Pittsburgh, PA, 1998.

(10) Schmidt, M. W.; Baldridge, K. K.; Boatz, J. A.; Elbert, S. T.; Gordon, M. S.; Jensen, J. H.; Koseki, S.; Matsunaga, N.; Nguyen, K. A.; Su, S. J.; Windus, T. L.; Dupuis, M.; Montgomery, J. A. *J. Comput. Chem*. **1993**, *14*, 1347.

(11) (a) Møller, C.; Plesset, M. S. *Phys. Rev*. **1934**, *46*, 618. (b) Binkley, J. S.; Pople, J. A. *Int. J. Quantum. Chem*. **1975**, *9*, 229.

(12) (a) Ditchfield, R.; Hehre, W. J.; Pople, J. A. *J. Chem. Phys*. **1971**, *54*, 724. (b) Hehre, W. J.; Ditchfield, R.; Pople, J. A. *J. Chem. Phys*. **1972**, *56*, 2257. (c) Hariharan, P. C.; Pople, J. A. *Theor. Chim. Acta* **1973**, *28*, 213. (d) Francl, M. M.; Pietro, W. J.; Hehre, W. J.; Binkley, J. S.; Gordon, M. S.; DeFrees, D. J.; Pople, J. A. *J. Chem. Phys*. **1982**, *77*, 3654. (e) Clark, T.; Chandrasekhar, J.; Spitznagel, G. W.; Schleyer, P. v. R. *J. Comput. Chem*. **1983**, *4*, 294.

(13) Becke, A. D. *J. Chem. Phys*. **1993**, *98*, 5648.

(14) Lee, C.; Young, W.; Parr, R. G. *Phys. Rev*. **1988**, *B37*, 785.

(15) (a) Cizek, J. *J. Chem. Phys*. **1966**, *45*, 4256. (b) Pople, J. A.; Krishnan, R.; Schlegel, H. B.; Binkley, J. S. *Int. J. Quantum. Chem*. **1978**, *14*, 545. (c) Bartlett, R. J.; Purvis, G. D. *Int. J. Quantum. Chem*. **1978**, *14*, 561. (d) Purvis, G. D.; Bartlett, R. J. *J. Chem. Phys*. **1982**, *76*, 1910. (e) Purvis, G. D.; Bartlett, R. J. *J. Chem. Phys*. **1987**, *86*, 7041.

(16) Krishnan, R.; Binkley, J. S.; Seeger, R.; Pople, J. A. *J. Chem. Phys*. **1980**, *72*, 650.

(17) (a) Nyden, M. R.; Petersson, G. A. *J. Chem. Phys*. **1981**, *75*, 1843. (b) Petersson, G. A.; Bennett, A.; Tensfeldt, T. G.; Al-Laham, M. A.; Shirley, W. A.; Mantzaris, J. *J. Chem. Phys*. **1988**, *89*, 2193. (c) Petersson, G. A.; Al-Laham, M. A. *J. Chem. Phys*. **1991**, *94*, 6081. (d) Petersson, G. A.; Tensfeldt, T. G.; Montgomery, J. A., Jr. *J. Chem. Phys*. **1991**, *94*, 6091. (e) Montgomery, J. A., Jr.; Ochterski, J. W.; Petersson, G. A. *J. Chem. Phys*. **1994**, *101*, 5900. (f) Ochterski, J. W.; Petersson, G. A.; Montgomery, J. A., Jr. *J. Chem. Phys*. **1996**, *104*, 2598.

(18) Andrae, D.; Haeussermann, U.; Dolg, M.; Stoll, H.; Preuss, H. *Theor. Chim. Acta* **1990**, *77*, 123.

(19) (a) Fukui, K. *Acc. Chem. Res*. **1981**, *14*, 363. (b) Gonzalez, C.; Schlegel, H. B. *J. Chem. Phys*. **1991**, *95*, 5853. (c) Gonzalez, C.; Schlegel, H. B. *J. Chem. Phys*. **1989**, *90*, 2154. (d) Gonzalez, C.; Schlegel, H. B. *J. Phys. Chem*. **1990**, *94*, 5523.

(20) Wiberg, K. B. *Tetrahedron* **1968**, *24*, 1083.

(21) Reed, A. E.; Curtiss, L. A.; Weinhold, F. *Chem. Rev*. **1988**, *88*, 899.

(22) (a) Moyano, A.; Pericàs, M. A.; Valentí, E. *J. Org. Chem*. **1989**, *54*, 573. (b) Lecea, B.; Arrieta, A.; Roa, G.; Ugalde, J. M.; Cossío, F. P. *J. Am. Chem. Soc*. **1994**, *116*, 9613.

(23) (a) Morao, I.; Lecea, B.; Cossío, F. P. *J. Org. Chem*. **1997**, *62*, 7033. (b) Cossío, F. P.; Morao, I.; Jiao, H.; Schleyer, P. v. R. *J. Am. Chem. Soc*. **1999**, *121*, 6737.

(24) Bader, R. F. W. *Atoms in Molecules*: *A Quantum Theory*; Oxford University Press: Oxford, U.K., 1990.

(25) Biegler-König, F. W.; Bader, R. F. W.; Tang, T.-H. *J. Comput. Chem*. **1982**, *3*, 317.

(26) (a) Schwenke, D. W.; Truhlar, D. G. *J. Chem. Phys*. **1985**, *82*, 2418. (b) Frisch, M. J.; Del Bene, J. E.; Binkley, J. S.; Schaefer, H. F., III. *J. Chem. Phys*. **1986**, *84*, 2279.

(27) Tomasi, J.; Persico, M. *Chem. Rev*. **1997**, *94*, 22027.

(28) Barone, V.; Cossi, M. *J. Phys. Chem*. **1998**, *102*, 1995.

(29) Houk, K. N.; Gonzalez, J.; Li, Y. *Acc. Chem. Res*. **1995**, *28*, 81.

(30) (a) Houk, K. N.; Li, Y.; Evanseck, D. *Angew. Chem., Int. Ed. Engl*. **1992**, *31*, 682. (b) Dewar, M. J. S.; Jie, C. *Acc. Chem. Res*. **1992**, *25*, 537. (c) McCarrick, M. A.; Wu, Y.-D.; Houk, K. N. *J. Org. Chem*. **1993**, *58*, 3330, and references therein.

(31) (a) Huisgen, R. *J. Org. Chem*. **1976**, *41*, 403. (b) Houk, K. N.; Sims, J.; Duke, R. E., Jr.; Strozier, R. W.; George, J. K. *J. Am. Chem. Soc*. **1973**, *95*, 7287. (c) Houk, K. N.; Sims, J.; Watts, C. R.; Luskus, L. J. *J. Am. Chem. Soc*. **1973**, *95*, 7301.

(32) (a) Fukuda, S.; Kamimura, A.; Kanemasa, S.; Hori, K. *Tetrahedron* **2000**, *56*, 1637. (b) Toma, L.; Quadrelli, P.; Perrini, G.; Gandolfi, R.; Valentin, C. D.; Corsaro, A.; Caramella, P. *Tetrahedron* **2000**, *56*, 4299. (c) Hu, Y.; Houk, K. N. *Tetrahedron* **2000**, *56*, 8239. (d) Nguyen, M. T.; Chandra, A. K.; Sakai, S.; Morokuma, K. *J. Org. Chem*. **1999**, *64*, 65. (e) Rastelli, A.; Gandolfi, R.; Amadè, M. S. *J. Org. Chem*. **1998**, *63*, 7425. (f) Houk, K. N.; Moses, S. R.; Wu, Y.-D.; Rondan, N. G.; Jäger, V.; Schohe, R.; Fronczek, F. R. *J. Am. Chem. Soc*. **1984**, *106*, 3880. (g) Hayakawa, T.; Araki, K.; Shiraishi, S. *Bull. Chem. Soc. Jpn*. **1984**, *57*, 2216. (h) Hayakawa, T.; Araki, K.; Shiraishi, S. *Bull. Chem. Soc. Jpn*. **1984**, *57*, 1643. (i) Komornicki, A.; Goddard, J. D.; Schaefer, H. F., III. *J. Am. Chem. Soc*. **1980**, *102*, 1763. (j) Hiberty, P. C.; Ohanessian, G.; Schlegel, H. B. *J. Am. Chem. Soc*. **1983**, *105*, 719. (k) McDouall, J. J. W.; Robb, M. A.; Niazi, U.; Bernardi, F.; Schlegel, H. B. *J. Am. Chem. Soc*. **1987**, *109*, 4642. (l) Su, M.-D.; Liao, H.-Y.; Chung, W.-S.; Chu, S.-Y. *J. Org. Chem*. **1999**, *64*, 6710.

(33) (a) Domingo, L. R. *Eur. J. Org. Chem*. **2000**, 2265. (b) Tanaka, J.; Kanemasa, S. *Tetrahedron* **2001**, *57*, 899. (c) Carda, M.; Portolés, R.; Murga, J.; Uriel, S.; Marco, J. A.; Domingo, L. R.; Zaragozá, R. J.; Röper, H. *J. Org. Chem*. **2000**, *65*, 7000. (d) Yeung, M. L.; Li, W.-K.; Liu, H.-J.; Wang, Y.; Chan, K. S. *J. Org. Chem*. **1998**, *63*, 7670. (e) Valentin, C. D.; Freccero, M.; Gandolfi, R.; Rastelli, A. *J. Org. Chem*. **2000**, *65*, 6112. (f) Liu, J.; Niwayama, S.; You, Y.; Houk, K. N. *J. Org. Chem*. **1998**, *63*, 1064.

(34) Avalos, M.; Babiano, R.; Bravo, J. L.; Cintas, P.; Jiménez, J. L.; Palacios, J. C.; Silva, M. A. *Chem. Eur. J*. **2000**, *6*, 267.

(35) (a) Domingo, L. R. *J. Org. Chem*. **1999**, *64*, 3922. (b) Vivanco, S.; Lecea, B.; Arrieta, A.; Prieto, P.; Morao, I.; Linden, A.; Cossío, F. P. *J. Am. Chem. Soc*. **2000**, *122*, 6078.

(36) Fabian, J.; Krebs, A.; Schönemann, D.; Schaefer, W. *J. Org. Chem*. **2000**, *65*, 8940.

(37) Ljubić,, I.; Sabljić, A. *J. Phys. Chem. A* **2002**, *106*, 4745.

(38) Neumann, F.; Lambert, C.; Schleyer, P. v. R. *J. Am. Chem. Soc*. **1998**, *120*, 3357.

(39) (a) Huisgen, R. *Angew. Chem., Int. Ed. Engl*. **1963**, *2*, 633. (b) Huisgen, R. *Angew. Chem., Int. Ed. Engl*. **1968**, *7*, 321. (c) Huisgen, R. *J. Org. Chem*. **1968**, *33*, 2291.

(40) (a) Firestone, R. A. *J. Org. Chem*. **1968**, *33*, 2285. (b) Firestone, R. A. *J. Org. Chem*. **1972**, *37*, 2181. (c) Firestone, R. A. *Tetrahedron* **1977**, *33*, 3009. (d) Firestone, R. A. *J. Chem. Soc. A* **1970**, 1570.

(41) (a) Kuznetsov, M. L.; Bokach, N. A.; Kukushkin, V. Yu.; Pakkanen, T.; Wagner, G.; Pombeiro, A. J. L *J. Chem. Soc., Dalton Trans*. **2000**, 4683. (b) Kuznetsov, M. L.; Dement'ev, A. I.; Shestakova, O. S.; Kukushkin, V. Yu. *Russ. J. Inorg. Chem*. **2001**, *46*, 1683. (c) Kuznetsov, M. L.; Kukushkin, V. Yu.; Haukka, M.; Pombeiro, A. J. L. *Inorg. Chim. Acta*, in press.

(42) (a) Sustmann, R. *Tetrahedron Lett*. **1971**, 2717. (b) Sustmann, R. *Tetrahedron Lett*. **1971**, 2721.

(43) (a) Smits, J. M. M.; Beurskens, P. T.; Smits, J. R. M.; Plate, R.; Ottenheijm, H. *J. Crystallogr. Spectrosc. Res*. **1988**, *18*, 15. (b) Eberson, L.; McCullough, J. J.; Hartshorn, C. M.; Hartshorn, M. P. *J. Chem. Soc., Perkin Trans. 2* **1998**, 41.

(44) Kuznetsov, M. L.; Nazarov, A. A.; Pombeiro, A. J. L.; Kukushkin, V. Yu. *New. J. Chem*., submitted for publication.

(45) Domingo, L. R.; Arnó, M.; Andrés, J. *J. Org. Chem*. **1999**, *64*, 5867.

(46) Charmier, M. A. J.; Kukushkin, V. Yu.; Pombeiro, A. J. L. *J. Chem. Soc., Dalton Trans*. **2003**, 2540.

(47) Hermkens, P. H. H.; Maarseveen, J. H. v.; Kruse, C. G.; Scheeren, H. W. *Tetrahedron* **1988**, *44*, 6491.